Radjabian, M.; Koll, J.; Buhr, K.; Handge, U.A.; Abetz, V.:
Hollow Fibre Spinning of Block Copolymers: Influence of Spinning Conditions on Morphological Properties
In: Polymer (2013) Elsevier

DOI: 10.1016/j.polymer.2013.01.033

Hollow Fibre Spinning of Block Copolymers: Influence of Spinning Conditions on Morphological Properties

Maryam Radjabian, Joachim Koll, Kristian Buhr, Ulrich A. Handge, Volker Abetz*

Institute of Polymer Research, Helmholtz-Zentrum Geesthacht, Max-Planck-Strasse 1, 21502 Geesthacht, Germany

*Corresponding author: volker.abetz@hzg.de

Telefon: +49 4152 87 2461
Telefax: +49 4152 87 2499

Abstract

The self-assembly of block copolymers proposes interesting strategies for design and fabrication of ordered nano/microdomain structures. Recently, large attention has been given to the preparation of integral asymmetric flat sheet membranes with cylindrical domains forming an isoporous top layer. In this work, this strategy is extended to the formation of nanoporous hollow fiber membranes from polystyrene-*block*-poly(4-vinylpyridine) (PS-b-P4VP) solutions via phase inversion process. In this way, the self-assembly of block copolymers into an ordered morphology via solvent evaporation is combined with microdomain alignment by shear flow in the die. The influence of the experimental parameters on the morphology of the hollow fiber is discussed, such as solution concentration and viscosity, extrusion pressure within the spinneret and air gap distance between the spinneret and the precipitation bath (evaporation time). The evaluation of the surface morphology of the membranes by scanning electron microscopy (SEM) confirms the strong effect of shear flow and solution viscosity on the formation of nanoporous structures in hollow fiber spinning.
Keywords: Hollow fiber membrane Polystyrene-b-poly(4-vinylpyridine) Microphase separation

1. Introduction

New materials and procedures have been developed to present alternative routes for the preparation of well-ordered nanostructured membranes [1]. The self assembly of block copolymers offers an attractive strategy to fabricate nanoporous membranes by choosing appropriately designed block chemistries, compositions and processes [2]. Recently, block copolymer based membranes with nanoscale pores, high porosity, narrow pore size distributions, highly selective separation and tunable chemical and mechanical properties have received large attention both from the scientific and the application viewpoint [1]. Block copolymers consist of two or more chemically incompatible blocks that are covalently joined. They can self-assemble into a variety of periodic arrays of spherical, cylindrical, or lamellar microdomains depending on the volume fraction of the blocks [1-3]. In solution, microphase separation can also occur and the block copolymers assemble into micellar structures, depending on the thermodynamic incompatibility between their chemically dissimilar segments, the selectivity of the solvent and the polymer concentration [3].

From a nanotechnological viewpoint, the self-assembly of block copolymers into regular crystal-like structures is very interesting as length scales can be obtained, which are not so easy to achieve by other methods. Many techniques have been developed to induce the alignment and control of the arrangement of microdomains in block copolymer films by coupling with external fields [4]. Solvent evaporation is one of the strong directional fields to kinetically freeze nanostructures under proper preparation conditions. Cylindrical microdomains vertically orientated to the film surface are a result of the maximized solvent concentration gradient along the direction perpendicular to the surface [5-7]. The typical domain sizes of cylinders or gyroidal networks formed by block copolymers make them interesting candidates not only as templates for nanolithographic applications, but also for ultrafiltration membranes. Cylinders vertically aligned to the plane of a substrate are useful to fabricate nanochannel structures and isoporous membranes, while those parallel aligned to the plane of substrate are also motivating in nanolithography [8].

Thin film morphologies have been widely studied for numerous block copolymers and post treatment effects such as thermal or solvent vapor annealing to remarkably improve the ordering of block copolymer morphologies [5,9-12]. However, large scale defect-free block copolymer

morphologies with perfect periodic domain ordering are difficult to obtain without the application of, for example, external forces or a well-designed surface topography. Researchers have applied external force for alignment of cylindrical phase block copolymer bulk materials to achieve defect-free orientations and to control lateral ordering of the nanoscopic domains [13]. Recently, a few studies have focused on the effect of shear flow [14-16], solution extrusion [17], and solvent evaporation coupled with flow through a channel [7] to align cylindrical block copolymer domains in solution.

One of the straight forward and most important industrial procedures for fabrication of integral asymmetric membranes is the non-solvent- induced phase separation (NIPS), where a cast film of a polymer solution is immersed in a precipitation bath. Combined self-assembly of block copolymers with non-solvent induced phase separation, now referred to as the SNIPS method, directly enhances formation of uniform pore sizes in the selective layer of membranes [18]. This one step novel procedure was established a few years ago [19] to prepare a nanoporous asymmetric membranes of a PS-b-P4VP diblock copolymer. The well-ordered nanoporous structure on the top layer of the block copolymer membranes is achieved by controlling the kinetic factors influencing self-assembly prior to reaching the thermodynamic equilibrium state. More studies on integral asymmetric block copolymer membranes from the same type of block copolymer (PS-b-P4VP) have been reported since then [11,12] and the concept could be extended to other stimuli-responsive membranes like PS-b-P2VP [12] and also postfunctionalized block copolymer membranes [20].

Hollow fiber membranes are generally used in many membrane applications ranging from gas separation to microfiltration. Compared to other membrane configurations, the main advantage of hollow fiber geometry is that it provides a high ratio of membrane area to module volume, and therefore higher productivity per membrane module. However, formation mechanism for hollow fiber membranes in which the polymer solution is extruded through a spinneret into a nonsolvent bath is more complex than in the case of integral asymmetric flat sheet membranes because of a larger number of morphology controlling factors during processing and phase inversion. The hollow fiber membranes fabricated via phase inversion by two internal and external coagulants have an asymmetric structure with a thin separating layer on the both inner and outer surface. The internal coagulant controls the inner skin morphology, while the external coagulant controls the outer skin morphology [21,22]. The addition of another evaporation step prior to precipitation in

wet-phase inversion processes (dry/ wet phase inversion) improves preparation of defect-free and ultrathin skinned asymmetric membranes [23].

However, in dry-jet wet-spinning processes, other factors such as extrudate swell, relaxation, gravitation and spinning-line stress in the air gap region along the distance between spinneret and precipitation bath can influence the membrane morphology and performance. Two dominant factors, elongational and shear stresses have a dramatic effect on the polymer segmental orientation and relaxation at the outer surface of the fiber [24-28]. The rheology of many polymer solutions is associated with a non- Newtonian behavior such as shear-thinning [27]. The segmental orientation induced by the shear flow within the spinneret relaxes in the short air gap region if the elongational stress caused by gravity along the spin line is small. However, the elongational stress caused by gravity becomes more prominent with increasing air gap distance which might enhance the spin line orientation [24,28]. The defect-free thin skin with nanoscale pores in narrow-sized distribution can develop the performance of the resultant membranes in selectivity and permeability. Block copolymers are able to implement this superior facility by self-assembly of well ordered nanoscale domains on top of the skin layer.

In the present work, we focus on the self-assembly of asymmetric PS-b-P4VP diblock copolymers (where P4VP forms cylinders in the bulk morphology) during hollow fiber spinning. To our knowledge, our experiments for the first time establish the manufacturing of nanostructured hollow fiber membranes by phase inversion dry-wet jet spinning of diblock copolymers which form cylindrical morphology. In this way, the self assembly of block copolymers into an ordered morphology induced by solvent evaporation is coupled with the alignment of cylindrical domains through shear flow. The hollow fibers are spun from the concentrated solutions of PS-b-P4VP in different mixtures of solvents (THF and DMF). The block copolymer undergoes microphase separation at a certain solution concentration and composition during solvent evaporation. The influence of effective parameters of shear stress, solution viscosity and evaporation time on the formation of regular nanoporous structures in hollow fiber was evaluated by variation of the block copolymer concentration, the pressure gradient within the spinneret and air gap distance between the spinneret and the precipitation bath.

2. Experimental section

2.1. Material

ULTEM® 1000 Polyetherimide (PEI) resin purchased from General Electric Company, USA, was used in this study. The weight average molar mass, $M_w = 5.8 \times 10^4$, and $M_w / M_n = 1.92$ were determined by gel permeation chromatography (GPC) (Waters 2410 refractive-index detector) at 50 ^oC calibrated against polystyrene standards. N. N-dimethylformamide (DMF) and tetrahydrofuran (THF) were used as received.

2.2. Synthesis of PS-b-P4VP

PS-b-P4VP diblock copolymers with two different compositions were synthesized by sequential anionic polymerization following the procedure described elsewhere [19]. The polymerization of styrene as the first block was initiated with s-butyl lithium suspended in cyclohexane. After 2 h, 4-vinylpyridine monomer was added and the temperature of −62 ^oC was maintained for a further period of 2 h. The polymerization was quenched with argon saturated methanol. After the addition of a few crystals of 2, 6-di-*tert*-butyl-4-methyl-phenol (to prevent thermal decomposition), half of the THF was removed by distillation at reduced pressure. The block copolymer was obtained by precipitation of the solution into a 10- fold excess of a 1:1 (v/v) methanol/water mixture with a typical yield of 60-70% [19].

The PS-b-P4VP compositions were determined by means of 1H NMR spectroscopy in deuterated chloroform as solvent. 1H NMR spectra were recorded on a Bruker advance 300 NMR spectrometer at 300 MHz with internal standard DMSO-d6. The molecular weights of the precursors and molecular weight distributions were measured by GPC at 30 ^oC calibrated against polystyrene standards. Two different types of PS-b-P4VP diblock copolymers were used in this study which we refer to “PSP4VP-A” and “PSP4VP-B”. The molecular characteristics of the block copolymers are listed in Table 1.

Table 1

PS-b-P4VP block copolymers characteristics.

Block copolymer code	Block copolymer type	Molecular weight (kg/mol)	Polydispersity index	P4VP content (wt %)
PSP4VP-A	$PS_{83.3}$-b-$P4VP_{16.7}$	198	1.07	16.7
PSP4VP-B	PS_{81}-b-$P4VP_{19}$	167	1.06	19.0

2.3. Production of hollow fiber membranes

The copolymers were dissolved in mixtures of DMF and THF at room temperature for about 24 h under agitation with a magnetic stirrer to form homogeneous solutions. The copolymer solutions at different concentrations and solvent mixtures were stored at room temperature without disturbance for 12 h to remove the shear effect of stirring and fine air bubbles entrapped in the solutions.

The hollow fiber membranes were fabricated by a well-known dry-jet wet-spinning process. A bore fluid was fed into the spinneret with an inner diameter of 0.212 mm, a die gap of 0.1745 mm and a die length of 1 mm. The dope solutions were dispensed under nitrogen pressure into the annulus of the spinneret at a controlled rate and went through an air gap area. Then fibers were subjected to non-solvent-induced phase separation before they were dried. Water was used as the bore fluid as well as the external coagulant in the immersion bath to produce integral asymmetric hollow fiber membranes by the phase inversion method. Variation in the air gap distance leads to different levels of THF evaporation because of the different times before precipitation of spun fibers in water occurs. The evaporation of DMF as the much less volatile solvent is negligible at these short times. As a result, the effect of elongational stress and gravity on the fiber formation as well as self-assembly cannot be ignored. The as-spun fibers were rinsed in flowing water at room temperature to complete removal of residual DMF, and then finally dried in the vacuum oven at 60 ^{o}C for more than 24 h.

2.4. Viscosity measurements

Rheological measurements of copolymer solutions were carried out at 20 °C with a laboratory rheometer (RC20-CPS). A cone-and-plate fixture was used with a plate diameter of 25 mm and a cone angle of 1 rad. The range of shear rates was 40-2500 s^{-1}.

2.5. Hollow fiber membrane characterization

The outer and inner skin layers and the cross section morphology of the hollow fiber membranes were evaluated by scanning electron microscopy (SEM) (LEO 1550VP Gemini from Carl ZEISS) at a potential of 5 kV. The hollow fibers were freeze fractured under liquid nitrogen,

which gave a generally clean fracture surface. The sample surface was coated with a thin layer of Pt by sputtering in a vacuum evaporator.

3. Results and discussion

3.1. Rheological properties of block copolymer solutions

Fig. 1 displays the dynamic viscosity of the PEI and PS-b-P4VP solutions versus shear rate. PEI was used for comparison, as it is a typical material used for hollow fiber membranes. The flow dependency behavior of the block copolymer solutions differs significantly from the homopolymer solution. For the PEI solution, the viscosity is not considerably affected by the shear rate and almost constant for the measured shear rates (Newtonian behavior). On the contrary the concentrated diblock copolymer solutions are strong shear-thinning power law fluids in the accessible range of shear rates. The slope of the linear curves on a double logarithmic-scale determined by a power-law fit varies in the range of 0.4-0.6. The reduction of the viscosity reflects structural changes at the applied stresses. These structural changes may be the result of the domain deformation or domain alignment into the flow direction.

It was found that both polymer concentration and solvent composition may exhibit a strong influence on the orientational response of the block copolymers [17]. As can be seen in Fig. 1 the dependence of the solution viscosity on the shear rate is influenced by the molecular weight and the different weight fractions of the blocks in addition to the solvent composition. An increase of the concentration considerably increases the solution viscosity in the accessible range of shear rates. However, the variation of the slope of the viscosity function was not remarkably affected by the solvent composition and solution concentration.

In block copolymer systems, there are additional enthalpic interactions between unlike block segments. Repulsive interactions force the system to undergo a disorder-to-order transition (DOT) with increasing copolymer concentration. However, shear flow can have a significant effect on this transition [15]. A shear-induced order-to-disorder transition (ODT) has been observed [29] for shear rates higher than the critical one needed to achieve a shear-induced disorder-to-order transition. In concentrated solutions, a drop in viscosity with shear rate can result from rearrangement or transformation of the initial structure to a highly oriented structure and finally complete destruction of the lattice network at a critical stress. Therefore the reduction in the viscosity is due to the reduced interactions between neighboring micelles. The critical

stress, at which shear induced disordering of the microphase separated structure happens, significantly decreases by decrease of the block copolymer concentration [15].

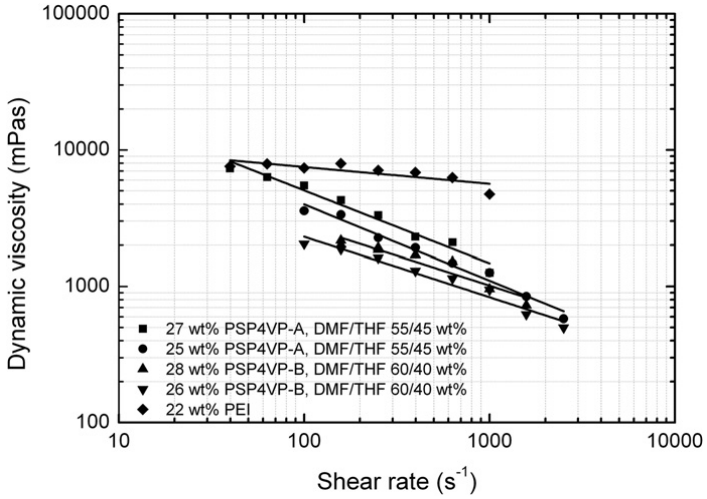

Fig. 1. Dynamic viscosity η versus shear rate $\dot{\gamma}$ of the PEI and PS-b-P4VP solutions measured at 20 °C.

3.2. Morphology of block copolymer hollow fiber membrane

The hollow fiber membranes were prepared from a 27 wt% PSP4VP-A copolymer solution in a mixture of DMF/THF (55/45 wt%) at different spinning conditions. The solution-cast film on a flat porous substrate shows perpendicularly aligned and hexagonally packed cylinders on the top layer of the porous support. Fig. 2 shows scanning electron micrographs of the cross-section and inner surface of the fiber spun at 1 bar pressure, 90 cm air gap distance and bore fluid flow rate of 0.6 ml/min. In all scanning electron micrographs, the abbreviations of EP, AGD and BF correspond to the extrusion pressure, air gap distance and flow rate of bore fluid, respectively. As can be observed, the fiber shows a circular shape in the lumen with a regular inner layer. The cross-section exhibits different layer morphologies; dense inner skin layer, finger-like macrovoids layer near the inner edge and sponge like structure between macrovoids layer and thick dense outer skin. The shear flow in the die aligns the block copolymer microdomains into the shear direction. The domain orientation induced by the shear inside the spinneret is quickly frozen into a solidified skin by immediate precipitation because of getting in contact with the bore fluid water when leaving the spinneret. (see Fig. 2(b)). The fast formation of the dense inner skin layer can prevent structural rearrangement which leads the aligned domains in the fiber axis direction form the close-packed oriented structure on the internal skin. Consequently, the

exchange “or diffusion” rate of the solvent and non-solvent is reduced during the phase inversion process on the inner side of the hollow fiber.

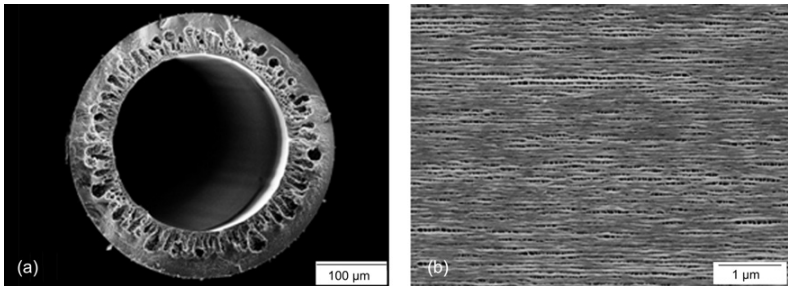

Fig. 2. SEM micrographs of (a) cross-section and (b) inner surface of the hollow fiber membrane prepared from a 27 wt % PSP4VP-A solution in a mixture of DMF/THF (55/45 wt %), EP=1 bar, AGD=90 cm and BF=0.6 ml/min.

The solvent evaporation process can produce highly ordered arrays of cylindrical microdomains oriented normal to the surface in self-assembled block copolymers [13]. This happens because of the gradient in the solvent concentration from the air interface into the inner part of the film during drying. It is noteworthy that solvents can change the relative concentrations of the blocks at the surface due to their selectivity [30]. Because of the low content of P4VP, in PSP4VP-A systems a higher amount of THF was chosen in the mixture of solvents to increase the solution viscosity as well as to decrease the solvent concentration profile with time. THF as a selective solvent for PS with higher vapor pressure is more likely to evaporate. It allows microphase separation to occur at the surface during solvent evaporation and a dense skin is formed on the outer surface of fibers before immersion into the precipitation bath. However, in the fiber spinning system the variation of the air gap distance limits the amount of THF which can evaporate before immersion.

After microphase separation this leads to a faster freezing of the PS matrix, compared to the still highly swollen P4VP domains, which contain more DMF. As mentioned before, the variation of the air gap distance between the spinneret and precipitation bath leads to different amounts of THF to evaporate and therefore the precipitation leads to a freezing at different stages of the structure formation, coupled possibly with different levels of unrelaxed morphological stresses from the spinneret. Hence, fast evaporation of the solvent kinetically develops the perpendicular alignments of the self-assembling domains to the plane of the surface. On the other hand, the combination of solvent evaporation with shear and elongational stress as external fields can enhance the microdomain orientation parallel to the fiber surface. The shear rate within the

annular die attains the highest value at the walls of the spinneret. Enhancement of the extrusion pressure leads to an increasing shear stress as well as shear rate at the spinneret wall which may significantly influence the domains alignment. Although from the vapor-solution interface into the bulk, the solvent concentration increases, conversely, the viscosity may increase further going into the bulk caused by the low chain orientation. Therefore, increase of the chain orientation in the direction of the vapor-solution interface due to the viscosity reduction may suppress the formation of perpendicular aligned cylinders in the time scale of the evaporation in air gap.

Fig. 3 shows the scanning electron micrographs taken from the outer surface of the spun fibers under different extrusion pressures. Distributions of the average pore diameter and surface porosity of the samples are shown in Fig. 4. It is noteworthy that surface porosity, pore size distribution and shape of the nanoscopic domains are influenced by solution pressure and evaporation time of the solvent before immersion bath. At high shear stresses, only some evidence of disordered arrays of nanoscopic pores is observed on the top layer. As presented in Fig. 3(c), a decrease of extrusion pressure which is coupled by increasing the solvent evaporation time improves the fabrication of a nanoporous array on the surface and increases the surface porosity (Fig. 4(c)). At low shear rates, domains can reorder during relaxation of the flow in the air gap into a favorable orientation, while at high pressures and therefore high shear rates the solution viscosity significantly drops due to the shear alignment of the cylindrical microdomains and they cannot pack well into the hexagonal perpendicular order during solvent evaporation.

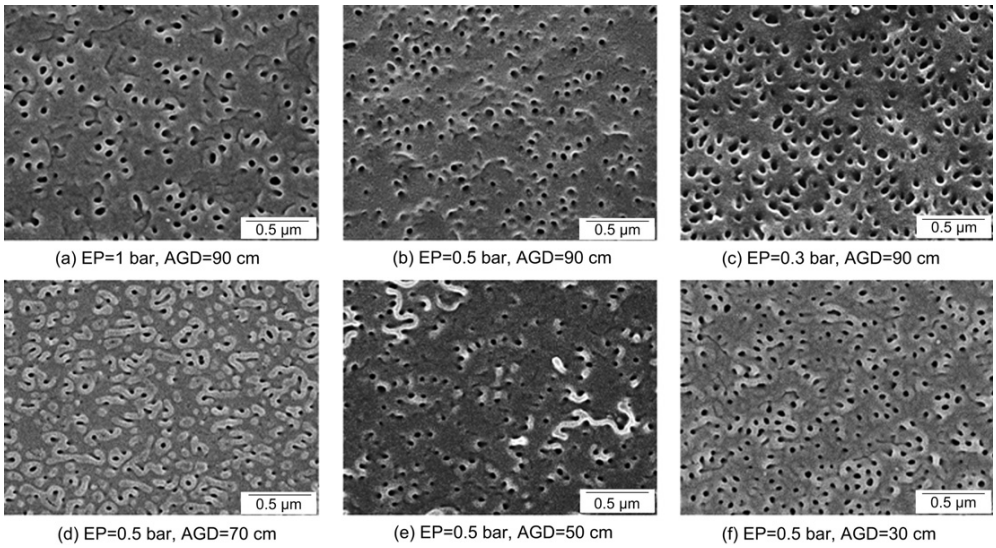

Fig. 3. SEM micrographs of the outer surface of the hollow fiber membranes prepared from a 27 wt % PSP4VP-A solution in a mixture of DMF/THF (55/45 wt %).

Fig. 3(b) and (d)-(f) also show the outer surface morphology of the nanoporous membranes spun at 0.5 bar polymer pressure at different air gap distances (90, 70, 50 and 30 cm). At this shear stress, controlling the degree of the solvent evaporation by variation in the air gap distance shows no significant effect on the ordering of the cylinders perpendicularly aligned to the surface. As a result, nanopores with a low degree of ordering were embedded in the polystyrene matrix and the collapsed pores are observed in some locations on the surface of the fibers. In addition, gravity may affect the shape of the pores, but this is not clearly supported by our results. Mutually destructive effect of the extensional stress caused by gravity and the shear stress may disturb the circular shape of the pores. However, it is noteworthy that coupling of these external forces with the self-assembly of the block copolymer during evaporation could not generate the optimized conditions to form a highly ordered nanoporous structure.

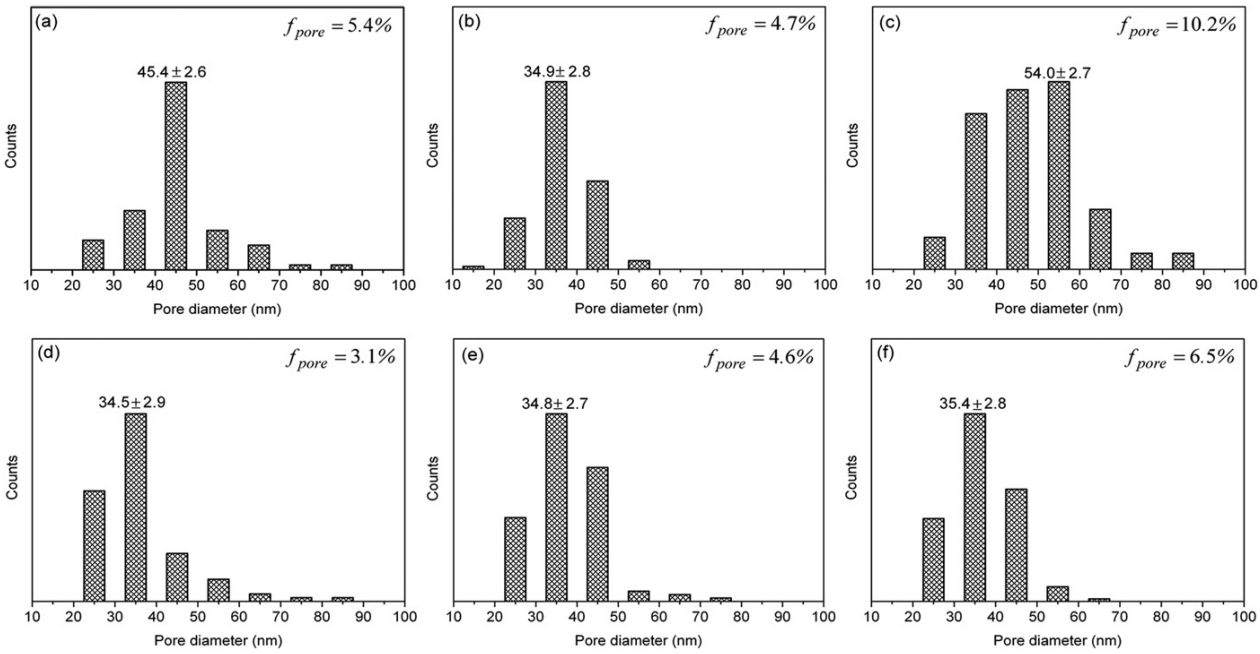

Fig. 4. Distribution of average pore diameter and surface porosity (f_{pore} %) of the outer surface of the hollow fiber membranes presented in Fig. 3.

To check the effect of block copolymer concentration on the formation of an isoporous surface morphology, the hollow fiber membranes were prepared from a 25 wt% and a 29 wt% PSP4VP-A solution in a mixture of DMF/THF (55/45 wt%). Figs 5 and 6 show the outer surface morphology of the hollow fiber membranes spun under the different spinning conditions from the above mentioned 25 wt%, an irregular morphology with large pores was detected by SEM on the outer surface of the membranes at different air gap distances. The absence of the well-ordered

nanoporous arrays on the top layer of the hollow fiber spun from the low concentration solution even at low shear stress reflects the strong dependence of the ordering transition and relaxation rate on the solvent concentration gradient. In this set of solutions the mobility of the block copolymer chains may be slightly too low due to the higher amount of fast evaporating THF compared to the solutions discussed further below. With time, lowest concentration of solvent at the surface directs microphase separation into the vertically ordered cylindrical arrays. While, the higher polymer mobility at the air interface due to the higher concentration of solvent, increases the tendency of formation of disordered domains with defects in the hexagonally packing of domains.

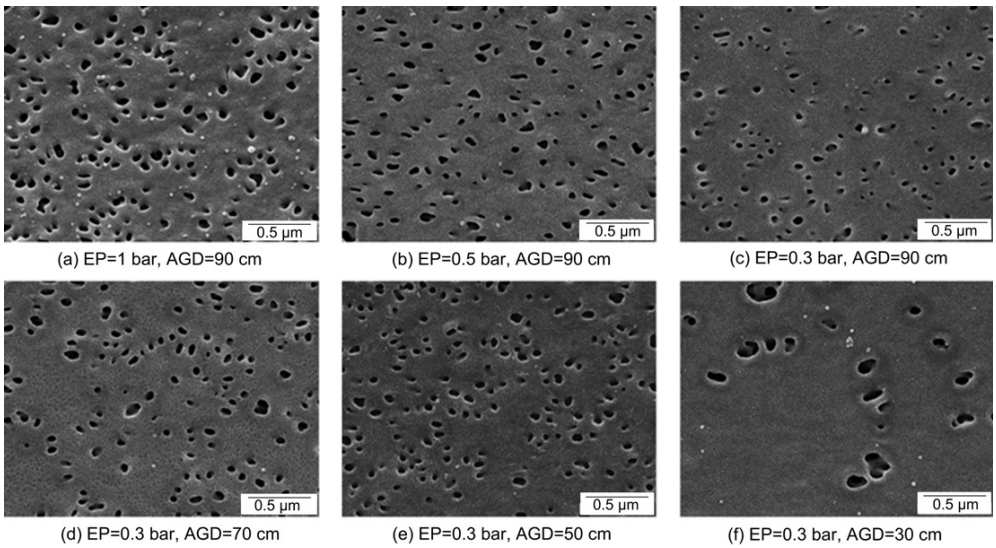

Fig. 5. SEM micrographs of the outer surface of the hollow fiber membranes prepared from a 25 wt % PSP4VP-A solution in a mixture of DMF/THF (55/45 wt %).

For the highly concentrated solution, 29 wt% PSP4VP-A, it was only possible to obtain hollow fibers under higher extrusion pressure. As can be seen in Fig. 6, a decrease in the solvent concentration also yields highly disordered arrays of nanopores on the outer surface of the membranes with low porosity at different air gap distances. It reflects that a uniform porous skin with fine pores alignment cannot be obtained by changing the evaporation time during spinning of the concentrated solution, because an increase in the polymer concentration is coupled with a decrease of the polymer mobility and enhancement of the shear stress necessary to enable a continuous spinning. Even if the solutions flow under the same profile of shear stress, a variation in the bulk solution concentration changes the relaxation behavior and solvent concentration gradient from the outer surface into the inner part of the fibers. In addition, the speed of spinning

is not the same even under the same shear stress due to the different viscosities of the solutions and therefore different shear rates. Consequently, the rate of solvent evaporation is different in the same air gap distance for different solutions spun under the same extrusion pressure. These results imply that an increase or decrease of the solvent concentration from 27 wt% could not drive the microphase separation of block copolymers to achieve the nearly defect-free arrays of nanopores on the skin layer of the fibers. It can be explained by decreasing or increasing of the relaxation rate normal to the direction of the vapor-solution interface which does not correspond to the time scale of evaporation to create a well-ordered self-assembled structure prior to the precipitation step.

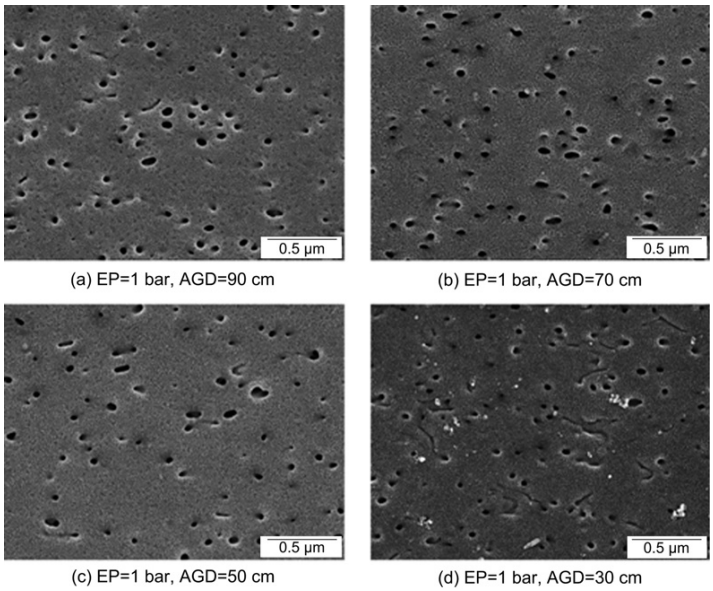

Fig. 6. SEM micrographs of the outer surface of the hollow fiber membranes prepared from a 29 wt % PSP4VP-A solution in a mixture of DMF/THF (55/45 wt %).

The effect of air gap distance, solution concentration and extrusion pressure on the outer diameter and wall thickness of the hollow fibers are presented in Fig. 7. Fig. 7(a) shows a significant effect of the higher extrusion shear flow on dimensions of the hollow fibers spun at the same flow rate of bore fluid. Decrease in viscosity occurs at high shear flow because of the non-Newtonian behavior of these fluids. Consequently, extrudate swelling of the increased dope extrusion leads to an increase of the inner and outer diameter of the fiber. However, lumen side coagulation on the extrusion flow and gravitational force in a certain air gap distance reduces the extrudate swell. On the other hand, increasing the gravitational effects by increasing the air gap distance considerably decrease the outer diameter and wall thickness of the hollow fibers (see

Fig. 7(a)-(c)). Besides, the experimental results show that dimensions of the fibers spun at constant conditions also depend on the viscosity of the dope solutions (Fig. 7(a) and (b)). An increase of the concentration (from 25 wt% to 27 wt%) and hence the viscosity of the solution which is coupled with a decrease of the shear rate as well as of the extrudate swell causes an increase of the outer diameter and wall thickness of the fibers.

The dependence of the cylinder orientation on the P4VP weight fraction was also investigated. Hollow fiber membranes were fabricated from another asymmetric PS-b-P4VP diblock copolymer, PSP4VP-B with a higher weight fraction of P4VP. Solution-casting a film of 26 wt% PSP4VP-B in a mixture of DMF/THF (60/40 wt%) forms highly ordered arrays of cylindrical domains oriented normal to the surface of a flat nonwoven substrate after precipitation. Compared to the PSP4VP-A solutions, because of the relatively higher content of P4VP in PSP4VP-B copolymer, less amount of THF was employed to achieve the well-ordered hexagonal packing of the cylinders. Fig. 8 presents the morphology of the outer surface of the fibers spun at different conditions. Distributions of the average pore diameter and surface porosity of the samples are presented in Fig. 9. The air gap distance also varied from 30 to 90 cm with 30 cm interval to change the evaporation time before immersion of the membranes into water. However at 1 bar extrusion pressure, no significant difference was observed in the measured times at different air gap distances and the solvent could evaporate between the spinneret and immersion bath around 2 s.

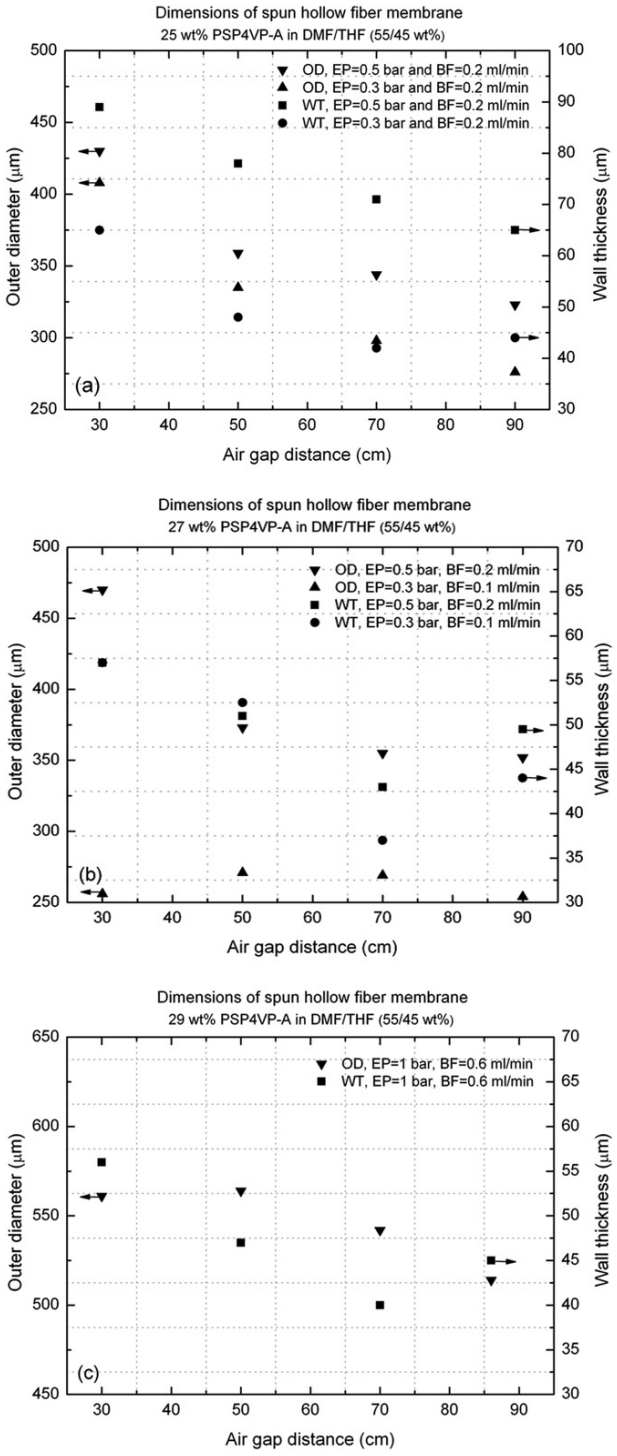

Fig. 7. Effect of air gap distance, solution concentration and extrusion pressure on outer diameter and wall thickness of the hollow fiber membranes prepared from 25 wt % (a), 27 wt% (b) and 29 wt % PSP4VP-A solutions in a mixture of DMF/THF (55/45 wt%). OD and WT refer to outer diameter and wall thickness, respectively.

In Fig. 8(a)-(d), the morphology of the nanoporous membranes consists of disordered networks of interconnected microdomains. The cylindrical domains are randomly oriented and it is difficult to observe any hexagonal order. The spun fibers show irregularly shaped pores and elongated worm like domains. However, under these conditions, the orientation of the cylinders somehow is a mixture of both perpendicular and parallel direction to the surface. The elongated worm like pores increase the surface porosity of the membranes and a much broader distribution was obtained (Fig. 9(a) and (d)). The creation of this three dimensional disordered network can be elucidated by the fast relaxation of the shear-induced structure coupled with lack of sufficient time for maximizing the solvent concentration gradient over the cross section to induce the well-ordered domains. Formation of the more ordered cylindrical domains is achieved by reducing the extrusion pressure which is coupled with an increase of the evaporation time (see Fig. 8(f)). The narrowest pore size distribution with the smallest average pore diameter was achieved for the fiber spun at lowest shear rate (Fig. 9(f)). In conclusion, modifying the spinning conditions of PSP4VP-B block copolymer gives the opportunity to achieve a less-defective ordered nanostructure on the fiber surface.

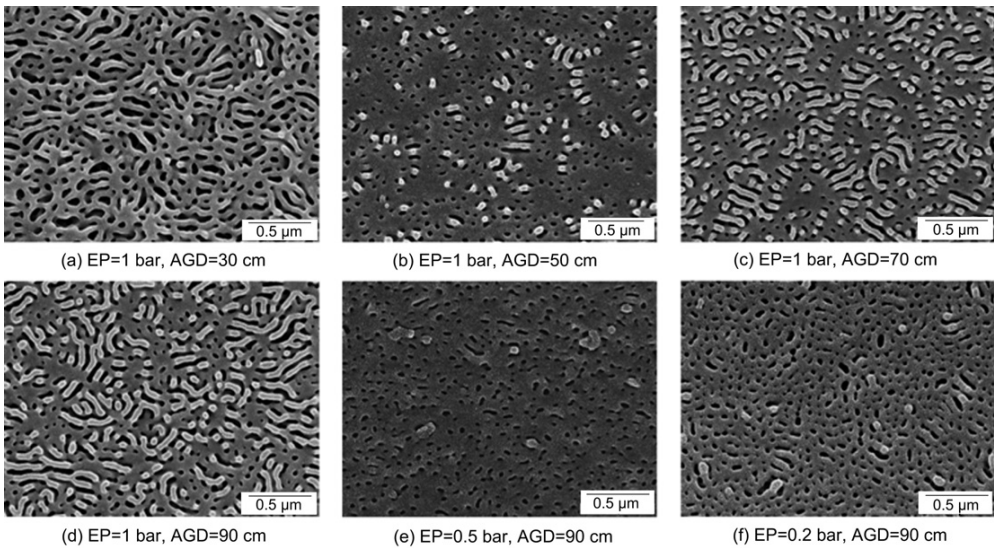

Fig. 8. SEM micrographs of the outer surface of the hollow fiber membranes prepared from a 26 wt % PSP4VP-B solution in a mixture of DMF/THF (60/40 wt %).

As for PSP4VP-A a similar study was made on the PSP4VP-B system to examine the effect of the block copolymer concentration on the ordering of the domains and orientation of the shear-induced structure. These experiments with another type of block copolymer somehow confirm

the above discussion regarding to the effect of polymer concentration on the self-organization of block copolymer fibers. The hollow fibers were prepared from a solution of 28 wt% PSP4VP-B in a mixture of DMF/THF (60/40 wt%) under different spinning conditions. The surface morphology of the fibers spun at two different air gap distances (30 and 90 cm) and under different pressures was evaluated by SEM (Fig. 10). Although the shear stresses within the spinneret were similar for both solutions, however, the more concentrated solution was spun at lower shear rates compared to the less viscous solution with lower concentration. It has a significant influence on the relaxation rates in addition to change the evaporation time at the same air gap distance. Therefore, the surface morphology of the fibers compared to their corresponding fibers spun at lower concentration (26 wt%) show more cylindrical pores vertically aligned to the plane of surface.

Extrusion of the solution at high shear rates which is coupled with the strong orientation of the polymer chains disturbs the regular formation of the cylindrical pores on the surface (see Fig. 10(a) and (d)). A decrease of the extrusion pressure leads to an increase of the porosity of the outer layer with smaller nanopores which are not assembled into a regular hexagonal pattern (Fig. 10(b) and (e)). However, at this concentration, a further decrease in the shear stress has a contrary effect on the porosity due to the stronger dependency of pores formation on the evaporation time (Fig. 10(c) and (f)). Increase of the evaporation time by reducing the speed of spinning allows fewer irregular nanopores to be formed on the skin layer.

In addition, the degree of the solvent evaporation and elongational effect of the gravity force on disordering the nanopores formation is controlled by variation of the air gap distance. For viscous solutions, a higher porosity with a disordered pore morphology was achieved on the top layer of the samples spun at the smallest air gap distance (see Fig. 10(a)-(c)). In this case, the lower concentration of the solvent at the air-solvent vapor interface leads to a vertical growth of the cylinders to the plane of the surface even in the shorter time scale of evaporation. Although it can improve nanoscale pore formation, a well-ordered cylindrical pattern on top of the surface is not formed.

In hollow fiber spinning, as the air gap distance increases, the gravity-induced radial outflow owing to the elongational drawing becomes more intensive. Then fibers will be stretched and become thinner [23]. During the evaporation time, the air gap distance inserts another extensional

force into the direction of the fiber axis which may influence the structural relaxation. Therefore, the oriented domains of block copolymer as a result of the shear stress within the spinneret coupled with the solvent evaporation in the air gap are elongated by drawing force. The direction of the gravity force may disturb the orientation and ordering of the cylinders which kinetically prefer to relax perpendicular to the surface. However, the coupling between the shear-induced morphology and the gravity force as the external field still needs to be explored. Although it was not possible to achieve a defect-free arrangement of the nanoscale domains on the surface of the fibers even at low shear stress, at least it allows the formation of cylinders vertical alignment.

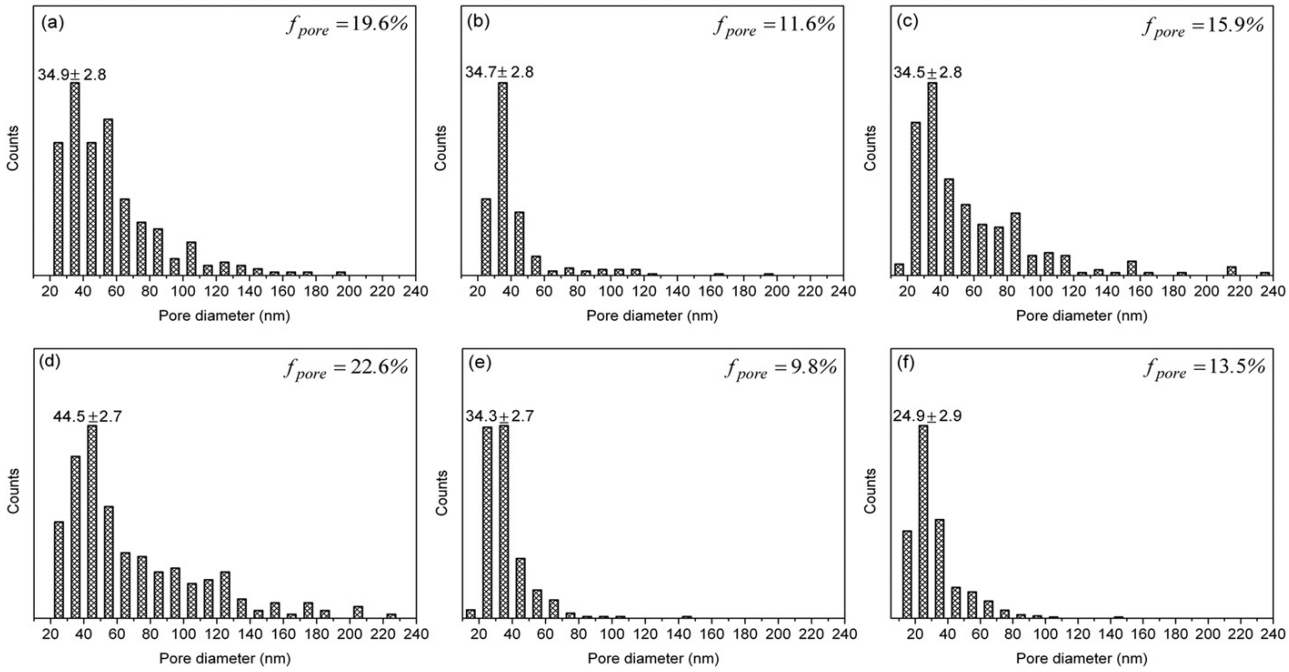

Fig. 9. Distribution of average pore diameter and surface porosity (f_{pore} %) of the outer surface of the hollow fiber membranes presented in Fig. 8.

Investigation of the effect of solution concentration (viscosity) and shear stress on the relaxation time and microdomain orientation is essential to understand the formation of a cylindrical pore morphology on the top layer. In the absence of shear stress, the perpendicular orientation of the cylindrical domains results from the solvent concentration profile which can control the profile of polymer relaxation rate in addition to the strong unfavorable interactions between the blocks as a thermodynamic driving force [5,6]. The hexagonal packing of the cylindrical domains rapidly formed when the relaxation rate increases less rapidly with position than the driving force for microphase separation decreases whereas the parallel alignment of the

domains formed in the opposite state. Hwang and colleagues [7] revealed that in a block copolymer with cylindrical microdomains, the orientation of the cylinders varied along the radial direction of the cylindrical tube of the film solution-casting. Highly aligned hexagonal arrays of domains were formed with their cylindrical axis perpendicular to the tube axis close to the wall boundary, while randomly ordered microdomains were observed at the center of the tube. In their method there is a shear gradient perpendicular to the tube axis somehow similar to the shear profile within the spinneret.

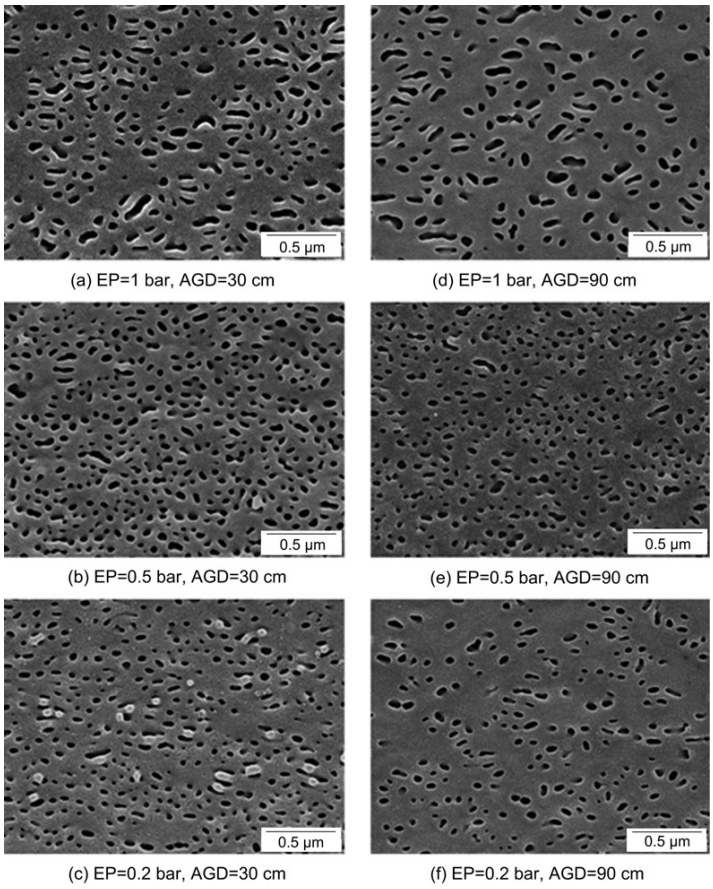

Fig. 10. SEM micrographs of the outer surface of the hollow fiber membranes prepared from a 28 wt % PSP4VP-B solution in a mixture of DMF/THF (60/40 wt %).

Hilliou and colleagues [15] performed rheo-optical experiments on semidilute asymmetric diblock copolymer solutions over a range of controlled shear stresses. They described the flow curve by five regimes as a function of shear stress. At low shear stress, the cylindrical micelles with isotropic orientations are not affected by the flow field as sufficient time is left for their relaxation under flow. At higher shear stress where anisotropic concentration fluctuations are enhanced along the flow direction, the domains are effectively deformed and forced to align

along the flow [15] as the characteristic time of the shear flow is faster than the relaxation time of the concentration fluctuations. A drop in the viscosity is the result of the structural change taking place in this stress region (shear thinning regime). At the highest stress applied in this regime, a viscosity plateau (or minimum) signifies the shear-induced DOT, which is associated with the alignment of shear-enhanced cylinders in solution along the flow direction. At a higher stress regime, corresponding to a loss of structural order (in the flow direction) coupled with an increase in viscosity, a homogeneous solution results from the stress-induced breakup of unstable cylinders [15].

In our system as well, the alignment of the self-assembled pattern of block copolymers is controlled by the external forces. In the absence of shear stress, the initial PS-b-P4VP block copolymer solution is close to the borderline between homogeneously dissolved block copolymer chains and formation of micellar aggregates, before THF starts to evaporate. Upon evaporation, the block copolymer starts to microphase separate into randomly oriented domains. Under low shear stress, at small deformation force which does not lead to structural changes in the block copolymer network, the cylindrical domains are structured due to the transition from disordered to ordered domains and oriented parallel to the shear deformation direction. The shear stress performs as the thermodynamic driving force to enhance the possibility of hexagonal packing of the cylindrical domains in the direction of deformation. This developed structure under shear can be responsible for the viscosity drop which affects the profile of relaxation rate similar as diluting the solution. Based on the notable viscosity reduction of PS-b-P4VP flow, the shear-induced structure may relax at different rates depending on the shear rate.

4. Conclusion

We manufactured hollow fiber membranes with nanoscale pores on the external surface by spinning PS-b-P4VP block copolymer solutions through dry/wet phase inversion process. The self-assembly of block copolymers into the ordered morphology via solvent evaporation is coupled with the microdomains alignment through the shear flow in the spinneret. To our knowledge, this study for the first time investigates the possibility of nanoporous hollow fiber membranes production by the phase inversion process using cylindrical block copolymers in concentrated solutions. The influence of block copolymer composition, solution concentration (viscosity), polymer pressure within the spinneret and air gap distance between the spinneret and

the precipitation bath (evaporation time) on the surface morphology of the hollow fibers were analyzed with SEM. It was found that, the cylindrical domains are not well-ordered on the outer surface of the fibers under high shear stress, reduction in viscosity and fast solvent evaporation time. However, a decrease in the shear stress as well as an increase in the evaporation time improves the cylindrical orientation of block copolymers in the perpendicular direction of the surface plane.

Acknowledgment

The authors are grateful to Brigitte Lademann for synthesizing the block copolymers. Anne Schroeder is acknowledged for SEM investigations.

References

[1] Wu D, Xu F, Sun B, Fu R, He H, Matyjaszewski K. Chem Rev 2012;112: 3959-4015.
[2] Parka C, Yoon J, Thomas EL. Polymer 2003;44:6725-60.
[3] Smart T, Lomas H, Massignani M, Flores-Merino MV, Perez LR, Battaglia G. Nanotoday 2008;3:38-46.
[4] Darling SB. Prog Poly Sci 2007;32:1152-204.
[5] Phillip WA, Hillmyer MA, Cussler EL. Macromolecules 2010;43:7763-70.
[6] Kim SH, Misner MJ, Xu T, Kimura M, Russell P. Adv Mater 2004;16:226-31.
[7] Hwang J, Huh J, Jung B, Hong JM, Park M, Park C. Polymer 2005;46:9133-43.
[8] Segalman RA. Mater Sci Eng R 2005;48:191-226.
[9] Jackson EA, Hillmyer MA. ACS Nano 2010;4:3548-53.
[10] Nunes SP, Sougrat R, Hooghan B, Anjum DH, Behzad AR, Zhao L, et al. Macromolecules 2010;43:8079.
[11] Nunes SP, Behzad AR, Hooghan B, Sougrat R, Karunakaran M, Pradeep N, et al. ACS Nano 2011;5:3516-22.
[12] Jung A, Rangou S, Abetz C, Filiz V, Abetz V. Macromol Mater Eng. 2012;297: 970-8.
[13] Park S, Kim B, Xu J, Hofmann T, Ocko BM, Russell TP. Macromolecules 2009; 42:1278-84.
[14] Sebastian JM, Lai C, Graessley WW, Register RA. Macromolecules 2002;35: 2707-13.
[15] Hilliou L, Vlassopoulos D, Pispas S, Hadjichristidis N. Macromolecules 2008; 41:3328-38.
[16] Mykhaylyk OO, Parnell AJ, Pryke A, Fairclough JPA. Macromolecules 2012;45: 5260-72.
[17] Harada T, Bates FS, Lodge TP. Macromolecules 2003;36:5440-2.
[18] Nunes SP, Car A. Ind Eng Chem Res http://dx.doi.org/10.1021/IE202870Y.
[19] Peinemann KV, Abetz V, Simon PFW. Nat Mater 2007;6:992.
[20] Clodt JI, Filiz V, Rangou S, Buhr K, Abetz C, Höche D, et al. Adv Funct Mater http://dx.doi.org/10.1002/adfm.201202015.
[21] Culfaza PZ, Rolevinka E, Rijnb CV, Lammertinka RGH, Wesslinga MJ. Membr Sci 2010;347:32-41.
[22] Peng N, Widjojo N, Sukitpaneenit P, Teoh MM, Lipscomb GG, Chung T-S, et al. Prog Polym Sci 2012;37:1401-24.
[23] Widjojo N, Chung TS. Ind Eng Chem Res 2006;45:7618.

[24] Chung TS, Teoh SK, Lau WWY, Srinivasan MP. Ind Eng Chem Res 1998;37: 3930-8.
[25] Chung TS, Xu ZL, Lin W. J Appl Polym Sci 1999;72:379-95.
[26] Qin JJ, Chung TS. Membr Sci 2004;229:1-9.
[27] Ismail AF, Yean LP. J Appl Polym Sci 2003;88:442-51.
[28] Ismail AF, Mustaffar MI, Illias RM, Abdullah MS. Sep Purif Technol 2006; 49:10-9.
[29] Balsara NP, Dai HJ. J Chem Phys 1996;105(7):2942-5.
[30] Albert JNL, Epps TH. Mater Today 2010;13:24-33.